ATTACHMENT 3

Contributions to ITU Working Party 4A
Relating to Ku-Band Sharing Issues

INTERNATIONAL TELECOMMUNICATION UNION

RADIOCOMMUNICATION STUDY GROUPS

Delayed Contribution
Document 4A/254-E
15 April 1999
Original: English only

Received: 14 April 1999

United States of America

METHODOLOGY TO DESCRIBE CONTINUOUS CURVES OF LONG-TERM EPFD LIMITS AS A FUNCTION OF ANTENNA SIZE

1 Introduction:

This document describes a methodology for developing continuous curves of EPFD limits as a function of antenna size for the long-term interference regime. Long term interference is nominally characterized as interference caused by a NGSO satellite antenna main-beam and/or sidelobe transmitting into the sidelobes of the GSO earth station antenna. Since the sidelobe gains of GSO earth station antennas are constant over large variations in peak antenna gain, the long-term NGSO interference power into the GSO earth station will be the same regardless of antenna size. Therefore, setting a constant value of I_o/N_o as a long-term interference criteria will result in a consistent level of degradation for all antenna sizes of the GSO earth station. Continuous curves of long-term EPFD limits as a function of antenna size can be developed based on a constant value of I_o/N_o.

Section 2 describes the long-term interference mechanism. Section 3 provides the GSO earth station reference antenna pattern that JTG 4-9-11 agreed should be the basis for assessing NGSO interference into GSO systems. It is shown that the interference power spectral density, I_o, is essentially constant regardless of antenna size in the long-term interference regime. Section 4 then proposes a methodology for computing the long-term EPFD limits as a function of antenna size based on maintaining a constant value for I_o/N_o.

2 Long-term Interference Mechanism:

There are four interference scenarios that must be considered to determine the overall interference levels produced by an NGSO system into a GSO network:

- interference from the main-beam of the NGSO system antennas into the main-beam of the GSO system receiver (main-beam to main-beam interference),
- interference from the main-beam of the NGSO system antennas into the sidelobe of the GSO system receiver (main-beam to sidelobe interference),
- interference from the sidelobe of the NGSO system antennas into the main-beam of the GSO system receiver (sidelobe to main-beam interference) and
- interference from the sidelobe of the NGSO system antennas into the sidelobe of the GSO system receiver (sidelobe to sidelobe interference).

All proposed NGSO systems use some technique to avoid the main-beam to main-beam interference regime, and the side-lobe to side-lobe case results in a very low interference regime and can be ignored. This leaves two interference regimes that need to be considered.

The short-term interference regime is due to the NGSO satellite antenna sidelobe transmitting into the GSO receiver main-beam. This produces a high-power, short-term interference event. The short-term events occur when the NGSO satellite is transmitting and is inline between the GSO satellite and the GSO earth station.

The long-term interference regime is due to the NGSO satellite transmitting from the satellite antenna main-beam into the GSO earth-station antenna sidelobe. This produces a more constant level of interference, and does not have the higher-power peak interference events characteristic of the short-term interference regime.

Certain types of NGSO systems, of which USAKU-M1 is an example operate so that their interference to GSO networks are only in the long-term interference regime. They never produce the short-term, higher-level, interference events that are characteristic of the inline events. It is the long-term interference regime that is being considered in this document.

3 Interference Power to GSO Earth Stations

At the January 1999 meeting of JTG 4-9-11, a GSO earth station reference antenna pattern for assessing the interference from NGSO systems to GSO systems was agreed upon (JTG 4-9-11/TEMP/71-R1). Figure 1 shows plots of this antenna gain as a function of the angle off the antenna boresight (antenna discrimination angle) for the three antenna sizes considered in WRC-97 Resolution 130.

For off boresight angles between about 4° and 10°, the antenna gain is constant for all antenna sizes of 60 cm or greater. At angles of greater than 10°, there is a slight change of antenna sidelobe gain dependent on whether the D/λ of the antenna is greater or less than 100. (D/λ for the 60 cm antenna is less than 100. D/λ for the 3 and 10 meter antennas is greater than 100.) Therefore, if the minimum discrimination angle of the NGSO satellite is greater than about 4°, the interference power (also interference power spectral density, I_o) into the GSO earth station from a NGSO satellite will be essentially constant regardless of the GSO earth station antenna diameter.

All of the proposed Ku-band NGSO systems use GSO arc avoidance techniques that result in GSO earth station antenna discrimination angles of greater than 4°. Table 1 lists the discrimination angle of known Ku-band NGSO systems.

TABLE 1:

Minimum Discrimination Angle of NGSO Systems

System	Minimum Discrimination Angle
Skybridge	10°
Boeing	10°
Teledesic	21°
HughesLINK	
HughesNET	
Virgo	
Denali	
Rostelesat	

Setting a constant value of I_o/N_o as the interference criteria will result in a constant level of GSO system performance degradation regardless of GSO earth station antenna diameter. Additionally, this matches what physically happens in real systems. The performance degradation of a GSO network can be viewed as the loss in carrier-to-noise power due to the additional interference produced by the NGSO system, and can be shown as:

$$\frac{C}{N+I} = \frac{C}{N \cdot \left(1 + \frac{I_o}{N_o}\right)}$$

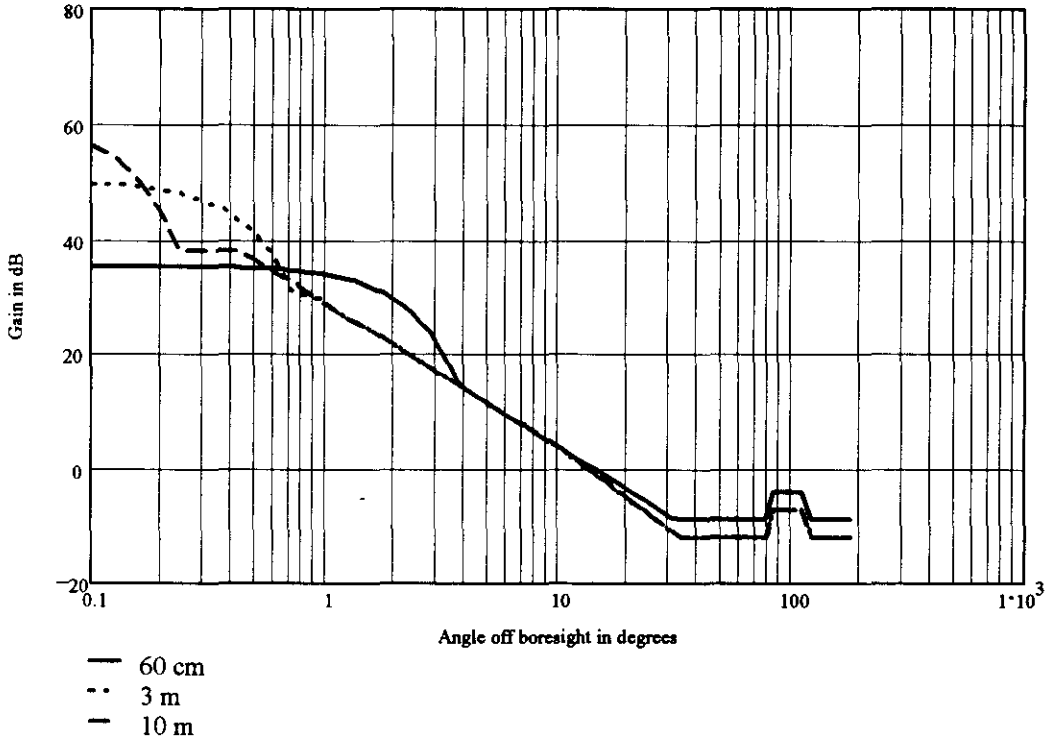

FIGURE 1:

GSO Earth Station Reference Antenna Pattern per JTG 4-9-11/TEMP/71-R1

4 EPFD Methodology

The EPFD can be calculated given the characteristics of the GSO earth station antenna and the level of interference power spectral density, I_o, produced by the NGSO system as follows:

$$EPFD = \frac{I_o \cdot BW_{ref}}{A_e}$$

where I_o is the interference power spectral density,

BW_{ref} is the reference bandwidth (BW_{ref} = 4 kHz for Ku-band), and

A_e is the effective area of the GSO earth station antenna.

The effective area of the antenna can be computed given the peak gain of the antenna and the frequency of the transmission.

$$A_e = \frac{G \cdot \lambda^2}{4\pi}$$

where G is the peak gain of the antenna, and

λ is the wavelength of the transmission.

The peak gain of the GSO earth station antenna can be determined from the equations given for G_{max} in the reference antenna pattern description.

$$G_{max} = 5.89 \cdot \left(\frac{D}{\lambda}\right)^2 \qquad \frac{D}{\lambda} < 100$$

$$G_{max} = 6.92 \cdot \left(\frac{D}{\lambda}\right)^2 \qquad \frac{D}{\lambda} > 100$$

The difference in the constant in the above equations for G_{max} is that different antenna efficiencies are assumed for electrically small antennas ($D/\lambda < 100$) and electrically large antennas ($D/\lambda > 100$). For the small antennas, the efficiency is assumed to be $\eta = 0.6$, and for the large antennas, the efficiency is assumed to be $\eta = 0.7$. Obviously the efficiency does not suddenly change as D/λ becomes greater than 100. However, for the purposes of this methodology, this discontinuity could be retained, or a smoothing function over some range of antenna sizes could be developed.

Rather than dealing with only the interference power spectral density, a more meaningful parameter is the ratio of interference power spectral density to noise power spectral density, I_o/N_o. The performance degradation for the GSO earth station is dependent on I_o/N_o.

$$\frac{C}{N+I} = \frac{C}{N \cdot \left(1 + \frac{I_o}{N_o}\right)}$$

Fixing a constant value of I_o/N_o to determine the long-term EPFD results in a consistent level of performance degradation for all sizes of GSO earth station antennas. Since

$$N_o = k \cdot T_{sys},$$

$$I_o = \frac{I_o}{N_o} \cdot k \cdot T_{sys}$$

where k is Boltzman's constant,

and T_{sys} is the effective noise temperature of the GSO earth station receive system.

Combining all this, an equation for EPFD is given as a function of the antenna diameter of the GSO earth station[1].

$$EPFD = 4\pi \cdot \frac{I_o}{N_o} \cdot kT_{sys} \cdot \frac{BW_{ref}}{5.89 \cdot D^2} \qquad \frac{D}{\lambda} < 100$$

$$EPFD = 4\pi \cdot \frac{I_o}{N_o} \cdot kT_{sys} \cdot \frac{BW_{ref}}{6.92 \cdot D^2} \qquad \frac{D}{\lambda} > 100$$

Figure 2 is a plot of the EPFD as a function of the antenna diameter for several values of I_o/N_o and a fixed T_{sys} = 188 °k.

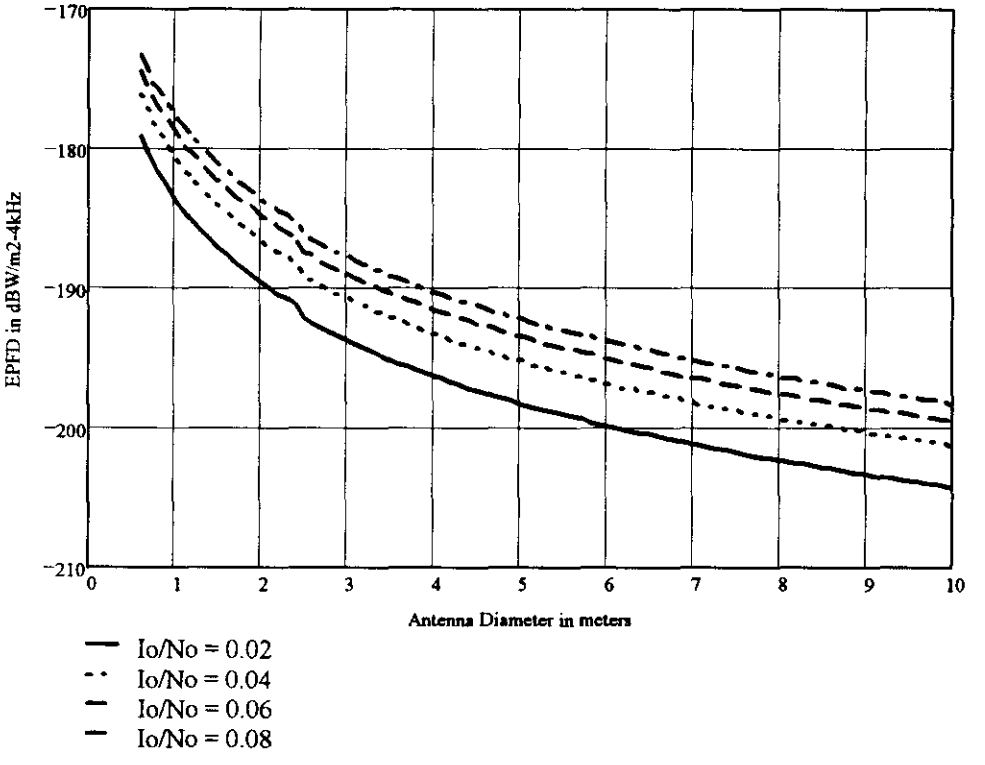

FIGURE 2:

EPFD as a Function of Antenna Diameter

[1] It should be noted that this formulation of the EPFD limit is independent of frequency, and can therefore be applied to any band.

5 Conclusions:

A methodology has been proposed for determining continuous curves of EPFD limits as a function of antenna diameter for long-term interference. The parameters of the function that would have to be agreed to are:

I_o/N_o, the ratio of interference power spectral density to noise power spectral density, and T_{sys}, the effective noise temperature of the GSO earth station.

This formulation for EPFD curves would provide consistency in the level of degradation that would be seen by different size GSO earth station antennas for long-term interference

INTERNATIONAL TELECOMMUNICATION UNION

RADIOCOMMUNICATION STUDY GROUPS

Delayed Contribution
Document 4-9-11/117-E
24 June 1998
Original: English only

Received: 23 June 1998

United States of America

STATISTICAL INVESTIGATION OF FADING ON THE DESIRED PATH RELATIVE TO FADING ON THE INTERFERING PATH

Introduction

Correlation of rain fading between two adjacent propagation paths is of concern when assessing allowable interference limits for satellite networks sharing the same frequency band. Under clear sky conditions the interference levels are set according to network performance requirements. Under degraded conditions the wanted and the interfering signals may not degrade by the same amount and a different interference level criteria must be used. In establishing such criteria the correlation of rain fading along the wanted path and the interfering path must be investigated. In general, rain cells extend over several kilometres and the correlation between fading along two paths through the same rain cell can be expected to be fairly high. At an earth station the interfering signal can arrive from different directions and the selectivity of the antenna pattern normally limits the angular region across which the interfering signal can enter the receiving system. This will also make the correlation between the wanted and the interfering signals to be relatively high. In the following, a general approach for deriving the correlation function for path attenuation between two propagation paths is presented. The fading difference between the two paths is further investigated by calculating a confidence level.

2 Path Attenuation Correlation Function

Figure 1 illustrates the path geometry for deriving the attenuation correlation function. It is assumed that the path length through rain extends up to the height, h_R, which is a function of the geographic latitude.

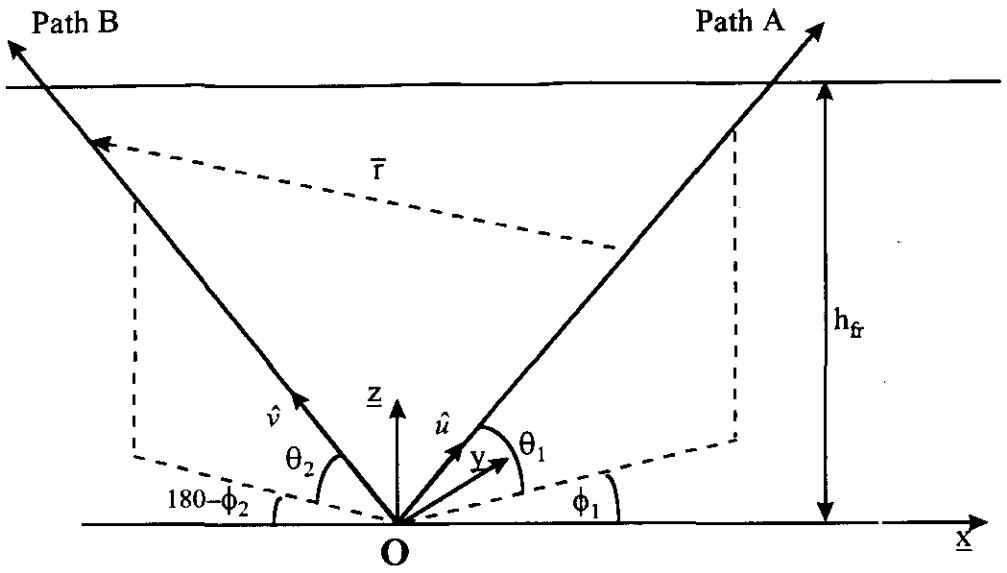

Figure 1: Propagation Path Geometry

The path attenuation can be expressed in terms of the specific attenuation using the integral:

$$A = \int_0^L \gamma \quad dl$$

$$\gamma = k R^{\alpha}$$

where γ is the specific attenuation, R is the rain intensity, L is the path length, and k and α are frequency-dependent coefficients (e.g. Recommendation ITU-R P.838).

It is assumed that the probability distributions of rain intensity follows the log-normal density function given by:

$$f(R) = \frac{1}{\sqrt{2\pi} R \sigma_R} \exp[-\frac{(\ln R - \mu_R)^2}{2\sigma_R^2}]$$

where μ_R is the mean value of R, σ_R is the standard deviation of R.

The path attenuation distribution is also found to follow approximately the log-normal distribution. Although the expression for the rain attenuation distribution given in Recommendation ITU-R P.618 does not have the log-normal form, predictions made with this procedure can be approximated by a log-normal fit with very good results. Figure 2 shows an example of such a fit. The attenuation distribution in Figure 2 corresponds to a frequency of 20 GHz, an elevation angle of 45°, a polarization angle of 45°, and the ITU rain zone K.

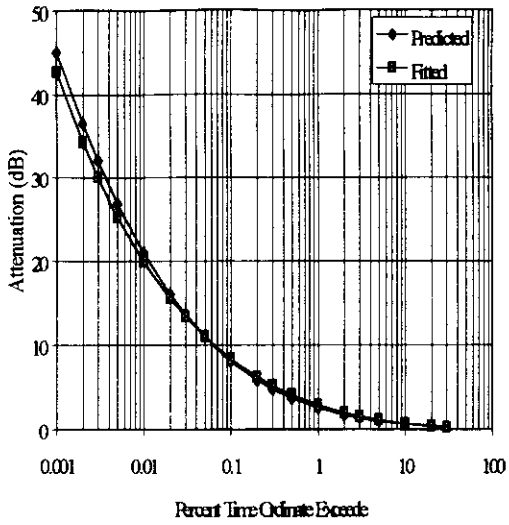

Figure 2: Log-normal Fit to the ITU Rain Attenuation Prediction

The joint probability density function for the path attenuations along the two paths can be expressed as:

$$f(A_a,A_b) = \frac{1}{2\pi\sigma_a\sigma_b A_a A_b\sqrt{1-c^2}} \exp\left(-\frac{1}{2(1-c^2)}\left[\frac{(\ln A_a-\ln \mu_a)^2}{\sigma_a^2} - 2c\frac{(\ln A_a-\ln \mu_a)(\ln A_b-\ln \mu_b)}{\sigma_a\sigma_b} + \frac{(\ln A_b-\ln \mu_b)^2}{\sigma_b^2}\right]\right)$$

where, σ and μ denote the standard deviation and mean of the log-normal distribution for attenuation for the individual paths, respectively, and c denotes the joint correlation coefficient:

$$c = \frac{\ln[\rho_A(a,b)\,(e^{\sigma a\sigma b}-1)+1]}{\sigma_a\sigma_b}$$

The correlation coefficient is related to the correlation function of the path attenuation $\rho_A(a,b)$ by:

$$\rho_A(a,b) = \frac{\int_0^{Da} ds \int_0^{Db} dt\rho\left(\left|s\vec{u} - t\vec{v}\right|\right)}{\left\{\left[\int_0^{Da} ds \int_0^{Da} dt\rho\left(\left|s-t\right|\right)\right]\left[\int_0^{Db} ds \int_0^{Db} dt\rho\left(\left|s-t\right|\right)\right]\right\}^{1/2}} = \frac{N(a,b)}{\Delta(a,b)}$$

where s and t are path lengths along the vectors $\vec{u}$ and $\vec{v}$ respectively. D_a and D_b are the path lengths up to the rain height .

The correlation function of path attenuation is a function of the spatial correlation function of specific attenuation given by kR^a. The coefficient a is close to 1 and therefore the specific attenuation correlation function can be approximated by the spatial correlation function of the rain intensity[1], $\rho(d)$. The correlation function for rain intensity has an exponential form, and is given by:

$$\rho = e^{-\alpha\sqrt{d}}$$

where α is a constant and d is the distance. A commonly used value for α is 0.25 with d expressed in km^2. Rain intensity correlation is assumed to be isotropic up to the rain height. With the use of the rain correlation function, the denominator of $\rho_A(a,b)$ reduces to[1]:

$$\Delta(a,b) = 2\sqrt{\tau(D_a)\,\tau\,(D_b)}$$

$$\tau(d) = \frac{2}{\alpha^2}\left(d + 2\left(d + \frac{3}{\alpha}(\sqrt{d} + \frac{1}{\alpha})\right)e^{-\alpha\sqrt{d}} - \frac{6}{\alpha^2}\right)$$

The numerator of $\rho_A(a,b)$ can be evaluated numerically using:

$$N(a,b) = \int_0^{Da} ds \int_0^{Db} dt\; e^{-\alpha\sqrt{r}}$$

where $r = |\vec{r}\,|$ and

$$\vec{r} = \underline{x}(D_a\cos\phi_1\cos\theta_1 - D_b\cos\phi_2\cos\theta_2) +$$
$$\underline{y}(D_a\sin\phi_1\cos\theta_1 - D_b\sin\phi_2\cos\theta_2) + \underline{z}(D_a\sin\theta_1 - D_b\sin\theta_2)$$

- θ_1 and θ_2 are the elevation angles of paths A and B, respectively
- ϕ_1 and ϕ_2 are the azimuth angles for paths A and B, respectively

Figure 3 shows the behavior of the attenuation correlation coefficient for two links originating at the same site as a function of the angular separation between the paths. The three curves shown corresponds to angular separation in elevation only, angular separation in azimuth only, and equal angular separation in both azimuth and elevation. The calculations are for a frequency of 20 GHz, latitude of 30° and rain zone K; the angular separation is taken with respect to an elevation angle of 45°.

The correlation coefficient, *c*, is also a function of the rain height and consequently the geographic latitude. However, the variation of *c* with latitude is relatively small as illustrated in Figure 4, where the same calculations in Figure 3 is repeated for 0° latitude.

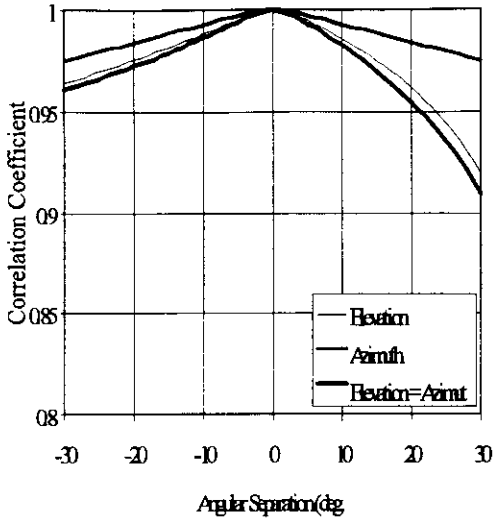

Figure 3. Dependence of Path Attenuation Correlation Coefficient on Angular Separation Between the Paths; 30° Latitude

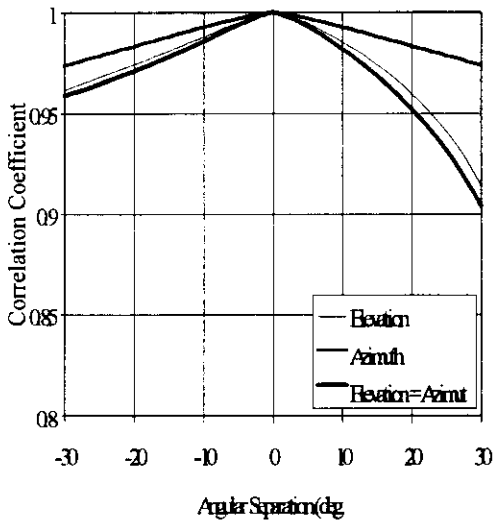

Figure 4. Dependence of Path Attenuation Correlation Coefficient on Angular Separation Between the Paths; 0° Latitude

The correlation coefficient shown in Figures 4 and 5 indicates only that the long term variations in the fading between the two paths are highly correlated. It gives no indication of how correlated the fading will be on an instantaneous basis. In order to gain some insight on the instantaneous correlation, the joint probability density function (derived earlier) was used to determine the confidence level that the fading difference between the two paths would be small.

The equation used to calculate this confidence level is

$$P(F_a - \varepsilon < F_b < F_a + \varepsilon) = \int_0^{F_a} \int_{F_a-\varepsilon}^{F_a+\varepsilon} f(A_a, A_b)\, dA_a\, dA_b$$

where F_a and F_b are fading limits on the desired and interfering paths, respectively. The equation calculates the probability that if the fading on the desired path is less than F_a then the fading on the interfering path is within ε of the desired fading.

Figures 5 through 7 show the confidence intervals when the fading on the desired path (F_a) is less than 3 dB, 5 dB and 10 dB. The frequency is 20 GHz, the earth station is at a latitude of 30° and the rain zone is K. The results are for an angular separation in elevation angle, only, and with respect to a desired elevation angle of 45°.

In general the figures show very high confidence that the interfering path will have approximately the same amount of fading as the desired path. Table 1 shows the minimum angular separation and confidence interval (ε) that corresponds to a 99% confidence level. Even with a 10 dB fade, there is a 99% confidence out to an angle of 3 degrees that the interfering fade will be within 0.25 dB of the desired signal.

Table 1: The minimum angular separation between the desired and interfering path that results in a 99% confidence level

F_a (dB)	ε (dB)	min angular separation (degrees)
3	0.25	3.6
3	0.5	8.4
5	0.25	3.0
5	0.5	7.2
10	0.25	2.8
10	0.5	6.4

Figure 5: Confidence level that the interfering fade is within ε of the desired fade, given that the desired fade is less than 3 dB

a)

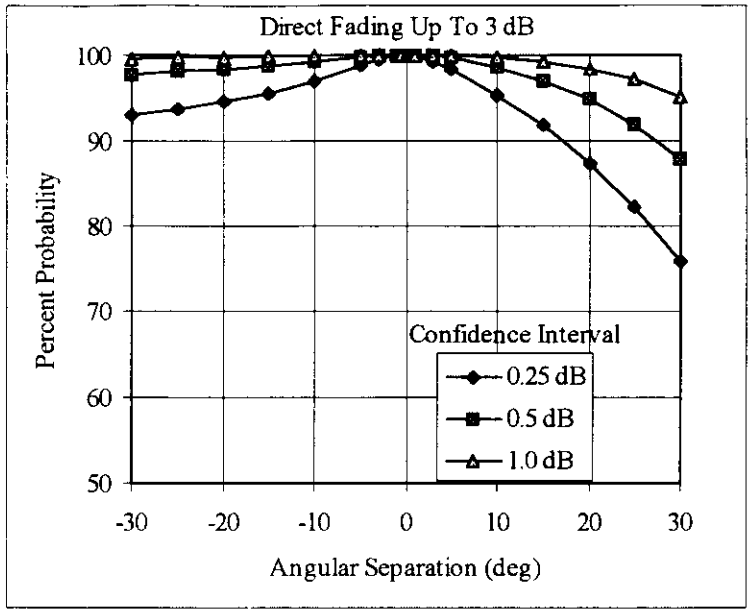

b)

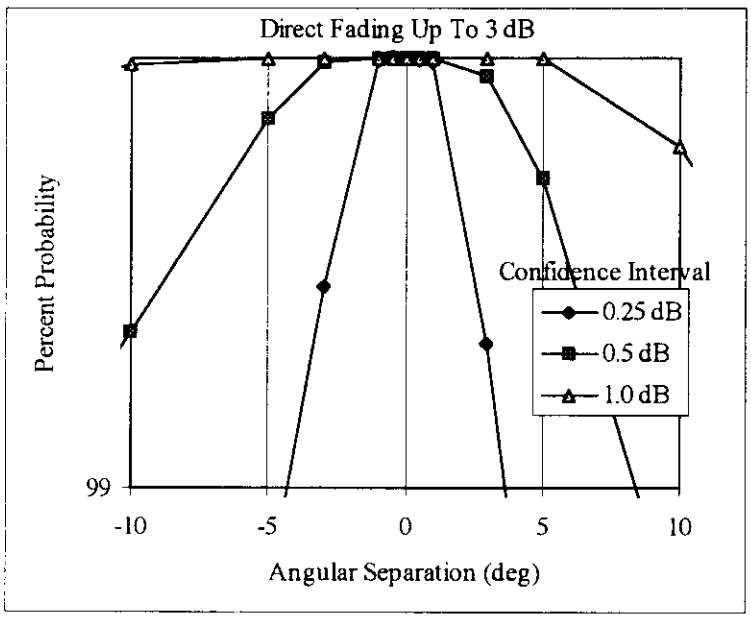

Figure 6: Confidence level that the interfering fade is within ε of the desired fade, given that the desired fade is less than 5 dB

a)

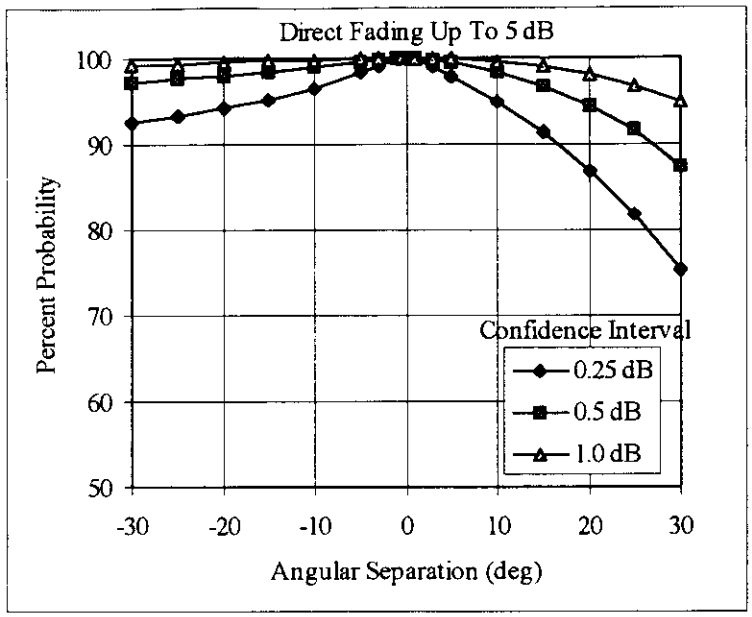

b)

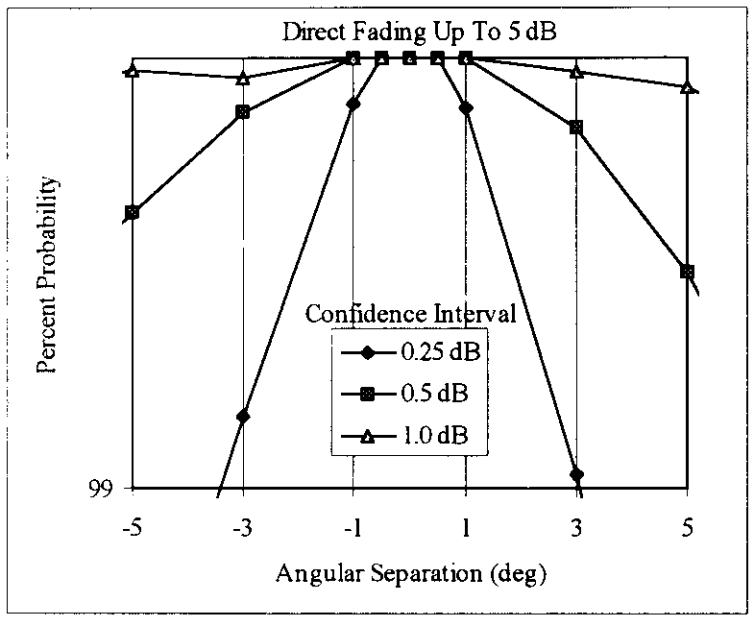

Figure 7: Confidence level that the interfering fade is within ε of the desired fade, given that the desired fade is less than 10 dB

a)

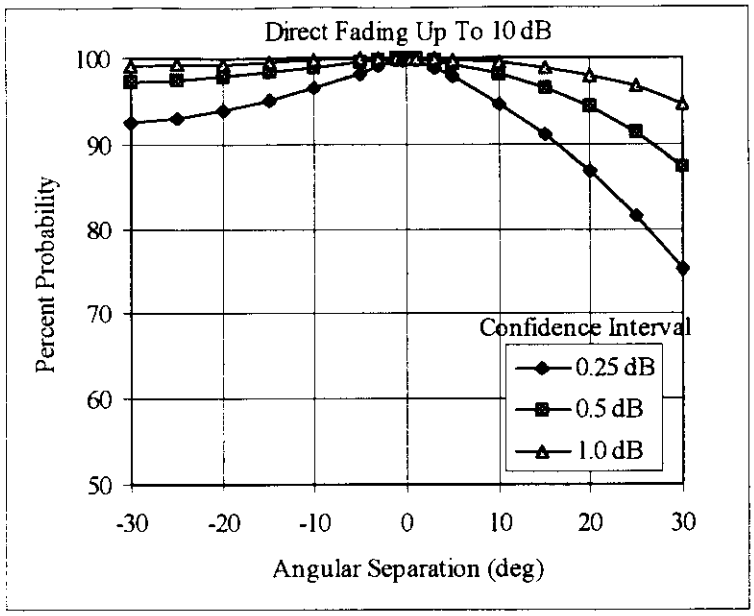

b)

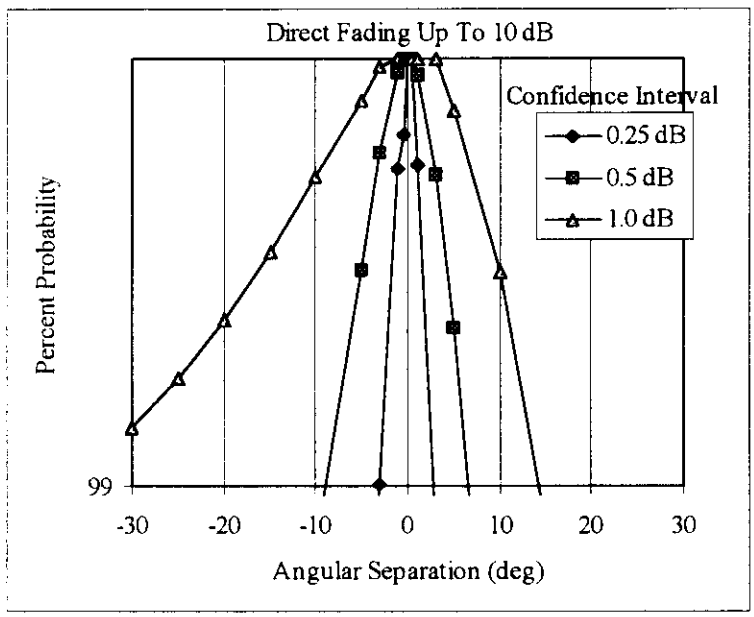

Discussion

The above results are not particularly sensitive to the earth station latitude, the intensity zone or the frequency. This is because only the means of the joint density function are affected. At Ku-band the probability of a given fading depth is lower. Therefore, the paths are correlated for a higher separation angle.

There are a lot of assumptions in the above analysis. Specifically it ignores the irregularities in the rain cells. This is true of some storms, but not true of others storms such as thunder storms.

For the above analysis to make any sense, the interfering and desired paths have to be within the same rain cell. Rain cells vary in size from a few kilometres to more than 10 kilometres. The path geometry is shown in Figure 8. If the desired signal elevation angle (θ), the distance to the edge of the rain cell (d), and the height of the rain cell (hfr) are known then the angle to the rain cell edge (γ) can be found.

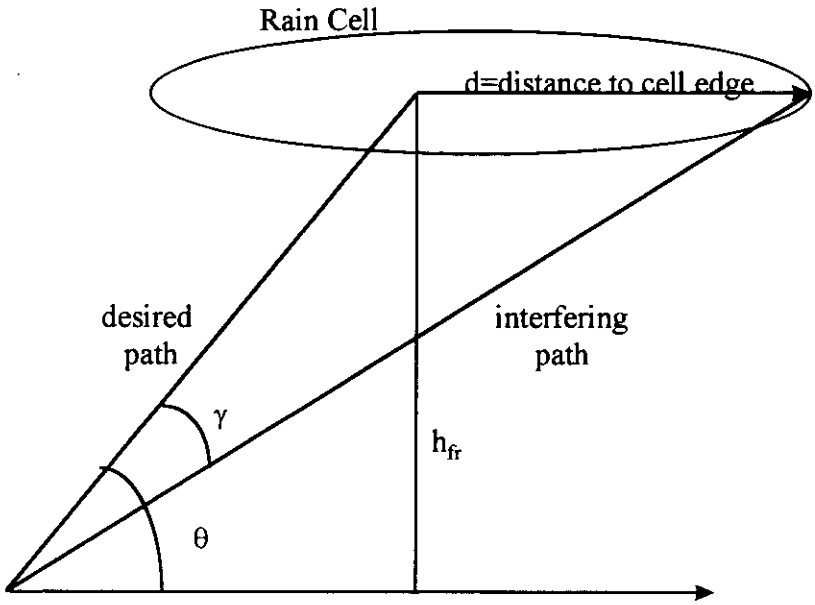

Figure 8: Rain cell geometry

Figure 9 is a plot of γ as a function of θ, given a rain height h_{fr}=4 Km. Two distances, d, were chosen to represent different cell sizes. It could be argued from Figure 9 and Table 1 that for elevation angles greater than about 20 degrees the fading on interfering and desired paths will be correlated when $\gamma < 3$ degrees.

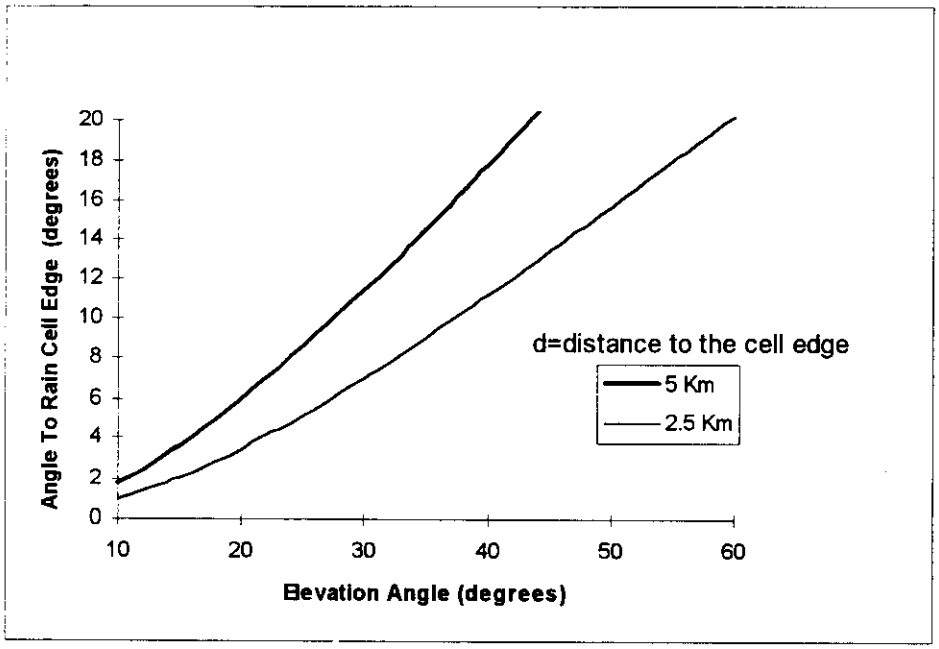

Figure 9: Angle from earth station boresight to rain cell edge versus earth station elevation angle

Rain Model Accuracy

Rain attenuation models generally fall into two classes: 1) those that attempt to define the physics of the process and model the constituents of storm cells, etc., and 2) those that use empirical approaches with simplified assumptions. For specific, narrowly focused programs - e.g. the development of a path attenuation model for a country or small region - approach number 1 has worked well, particularly if the country or region has the required input parameters for the model used. In general, it has been found that approach number 2 has the most global applicability. The key to approach number 2 is the development of a procedure that enables the user to move seamlessly from point rainfall rate to path average rainfall rate at any elevation angle. This is usually achieved by the introduction of an effective path length with an adjustment factor that gives the point-to-path averaging for the given look angle. Crane two component model is an example of the first approach and the ITU-R rain attenuation model is based on the second approach. Both models perform at a similar level with prediction accuracies on the order of 35% when compared with available measured attenuation data. In most cases the measured data pertain to single year measurements.

In general, the key contributory factors to the prediction uncertainty are:

- rainfall varies significantly from one year to the next and the associated year-to-year variability in the path attenuation can be as much as 20% of the long-term average
- lack of adequate characterization of rainfall in most parts of the world. The prediction accuracy tends to be better for those parts of the world where rainfall patterns are reasonably well understood; e.g. US, Europe, Japan.

Rain attenuation dominates over most other propagation effects at percentage times less than about 1%. At percent times above 1% other propagation factors such as clouds, melting layer and gaseous absorption must be considered. Their contribution towards the overall path attenuation can amount to several dBs at Ka-band and as much as 10 dB at V-band.

References

1. Morita, K., Higuti, I; Prediction of differential rain attenuation on adjacent microwave and millimeter wave links Rev. Elec. Comm. Labs., Vol. 25, pp. 96-103, 1977

2. Crane, R. K., *Electromagnetic Wave Propagation Through Rain* Wiley, New York, 1996

INTERNATIONAL TELECOMMUNICATION UNION

RADIOCOMMUNICATION STUDY GROUPS

Delayed Contribution
Document 4A/163-E
Document 4B/34-E
30 September 1998
Original: English only

Received: 30 September 1998

Subject: Resolution 130 (WRC-97), Question ITU-R 73/4

Source: Document 4A/TEMP/36, Section 5.0

United States of America

CONSIDERATIONS FOR HYPOTHETICAL REFERENCE DIGITAL PATHS WHEN IMPLEMENTED FOR PROVIDING SERVICES WHOSE AVAILABILITY ARE SENSITIVE TO SYNCRONIZATION TIMING RECOVERY

Introduction and purpose

WRC-97 made decisions allowing Non-Geostationary Satellite Orbit (NGSO) Fixed Satellite Service (FSS) systems to coexist with GSO FSS and Broadcast Satellite Service (BSS) systems operating in the Ku and Ka frequency bands. The conference adopted PFD limits to protect GSO systems from interference from NGSO-FSS systems. The conference also asked the ITU to review those limits, considering that the GSO arc must be protected to ensure continued use of existing FSS systems and the development of new GSO technologies and systems in both planned and unplanned bands.

Many FSS services are of a digital nature employing sequentially layered and synchronized coding schemes that address security, digital compression, and error correction and service applications. High levels of interference from NGSO systems, presumably corresponding to time allowance for unavailability, or even shorter periods of time could potentially result in the loss of synchronization of GSO communications which may in turn cause extended periods of service outage. Thus it is important to investigate synchronization performance of various GSO receivers and the attendant following operations and to determine the impact and the sensitivity to the levels of interference which may result from NGSO system operation.

The attached preliminary draft new Recommendation and its two Annexes provide a more detailed description of the issues as well means to resolve.

PRELIMINARY DRAFT PROPOSED NEW RECOMMENDATION

CONSIDERATIONS FOR HYPOTHETICAL REFERENCE DIGITAL PATHS WHEN IMPLEMENTED FOR PROVIDING SERVICES WHOSE AVAILABILITY ARE SENSITIVE TO SYNCRONIZATION TIMING RECOVERY

(Question ITU-R 73/4)

The ITU Radiocommunication Assembly,

considering

a) that the unavailability of a Hypothetical Reference Digital Path (HRDP) is determined by the combined effects of equipment and propagation availability;

b) that in some instances equipment unavailability is not due to equipment failure;

c) that Recommendation ITU-R S.521 specifies that HRDPs can include procedures such as: demodulation/modulation, error correction, buffer and processing which may be implemented in customer terminal or earth station equipment;

d) that HRDPs may implement the functions described in *considering* c) to provide services, such as MPEG-2, which contain sequentially layered coding schemes that may include among other things: address security, data compression, and error correction;

e) that such services, after loss of signal, may have a significant "time to recovery" after signal restoration;

f) that Recommendation ITU-R S.579 indicates that a service link, is considered to be unavailable when the received digital signal timing alignment (or synchronization) is lost for 10 consecutive seconds or more. Those 10 seconds are considered to be unavailable time and that period continues until timing alignment (or synchronization) are restored for 10 consecutive seconds;

g) that Recommendation ITU-R S.579 defines Availability and Unavailability of an HRDP link (which may include elements of *considering* c) as:

Unavailability = (unavailable time/required time) x 100%

Availability = (100% - unavailability);

h) that Annex 1 of this document will be taken into consideration,

recommends

a) that MPEG-2 and other services with similarly complex synchronization schemes take note that short periods of signal transmission loss due to propagation or interference can result in significant recovery times that should be taken into account when determining availability requirements;

b) that MPEG-2 and similar services, that are implemented on an HRDP link, have sufficient margin to sustain a BER of 1 part in 10^{10} over the full period of availability;

c) that MPEG-2 and similarly sensitive services, that are configured as in *recommends* 1 & 2, take measures in designing their links to ensure that statistical sources of interference will not cause additional equivalent link noise temperature increases in excess of 2.2 dB.

NOTE 1 – The time duration and frequency of occurrence of interfering signals can contribute to the determination of the allowable maximum interference level. It is observed that multiple short interference events can result in a larger increased period of unavailability than fewer long events (See Annex 2). This effect and the results of short duration (< 1 sec) interference events are subjects of further study.

ANNEX 1

CONSIDERATIONS FOR HYPOTHETICAL REFERENCE DIGITAL PATHS WHEN IMPLEMENTED FOR PROVIDING SERVICES WHOSE AVAILABILITY ARE SENSITIVE TO SYNCRONIZATION TIMING RECOVERY

1.0 Introduction and purpose

The synchronization behavior of several different classes of receivers were examined based on measurements performed or information supplied by earth station receiver manufacturers. The objectives of the investigation were to determine the interference duration and the power level required to cause the receiver to lose lock. For each receiver investigated, the degradation level and length of time necessary to cause loss of lock were determined. Additionally, the amount of time to reacquire lock for each receiver was determined. The results were then quantified so as to determine the synchronization loss criteria that could be applicable for all GSO FSS earth station receivers.

Table 1 provides a summary of the various types of receivers that were examined and tested. This is followed by an attachment describing, in detail, the tests conducted with accompanying results.

2.0 Digital video and audio receivers

2.1 MPEG-2 digital video and audio receiver

A typical MPEG-2 digital video and audio receiver is described in the attachment along with its performance and discussion of the test results. Performance measurements made on the MPEG-2 receiver demonstrate a synchronization loss margin, of 2.2 dB. An interference burst of approximately 1 to 2 seconds is required to cause complete loss of lock and the receiver reacquires 4 seconds after the interference ends.

The test results indicate that a satellite channel of the type tested above and implemented with margins that would protect during its availability to a threshold BER of 10^{-10} would lose lock if that margin were exceeded by 2.2 dB for a period of 1 to 2 seconds. Assuming operational levels were restored after loss of sync, the equipment would require an additional 4-8 seconds to return to normal operation.

3.0 Data receivers

Performance results for digital receivers operating at various data rates show that their synchronization loss margin is of the same order as discussed in Section 2.1. When the Eb/No falls below threshold and remains below it for a period of 1 to 2 seconds, it loses lock both frequency and data synchronization. The time duration to require lock depends on the particular algorithm used, and on the bandwidth that it must sweep in order to reacquire lock. Generally this is a function of the data rate, modulation method (BPSK, QPSK, etc.), coding/decoding method and the coding rate used. The total time to reacquire frequency and data lock varies from 10 to 15 seconds for moderate and high data rates up to the Mbit/s range and perhaps longer for early models operating in the kbit/s range.

4.0 Packet services

Packet data service may be affected for much longer periods even when a system abnormality lasts for a short duration.

The ITU-T considers a system to be unavailable after a service is unavailable for 10 seconds or more. The routing information for the packet service is updated every 30 seconds, and up to two cycles of such updating may be affected by a short abnormality and its after-effects. Thus, it may be concluded that although the receiver losses lock for only 1 to 15 seconds. The overall effect including the time for service restoration may be to make the service unavailable for much longer period.

5.0 On-board processing satellite networks

With the advent of on-board processing satellites, consideration of synchronization loss on the uplink of such networks must also be taken into account when evaluating the effects of interference from NGSO and other interference sources into GSO FSS systems. Further analysis will be necessary to determine the durations and levels of interference necessary to cause loss of lock at satellite receivers employing on-board processing.

6.0 Summary and conclusions

Test results of performance and interference susceptibility for several types of receiver-demodulators operating or planning to operate in the Ku and Ka bands have been completed. Additional information on other configurations and improvements in the state of the art is required.

Test measurements performed on typical digital receivers used for digital video, digital audio, and data service and voice applications indicate that noise or interference levels exceeding an operating threshold by **2.2** dB for 1-2 seconds or more will cause the receiver to lose sync. The tests demonstrate that when signals are returned to operational levels, after loss of synchronization, the receiver generally reverts to its initialization (scanning) state and may take up to 4 seconds before full synchronization is achieved. Then the remaining actions, relating to the content being received may take an additional 4-8 seconds to recover. It is apparent that further study on the time duration and frequency of occurrence of interference sources is required in order to fully quantify their effects on services with imbedded synchronization implementations.

For the systems tested it is apparent that service restoration time is an important factor that must be taken into consideration when determining the performance requirements of the service . Several factors affect the total time for which service restoration is required including: demodulator and bit synchronisation, frame synchronisation, error correction decoding, security synchronization, restoration of connection for voice circuits and re-initiation of transmission protocols for data circuits.

The results of test measurements for the receiver investigated are shown in Table 1.

TABLE 1

Summary of results of analysis of synchronization behaviour of different classes of earth station receivers

Receiver Type	Transmission Rate	Modulation Types	Code Types	Code Rates	Required BER	Eb/No (dB)	Degradation to Cause Lock *Loss*	Duration Degradation to Cause Lock Loss	Receiver Reacquisition Time	Total Time Lost Due to Loss of Lock	Other Effects
MPEG-2 Digital Video/Audio	2.5 to 15 Mbit/s	QPSK	Viterbi	1/2 2/3 3/4 5/6 7/8	10^{-10}	4.7 5.6 6.5 7.1 7.6	2.2 dB	1-2 seconds	4 seconds	4–12 seconds	
Rec/Demod #1	9.6 kbit/s to 2.336 Mbits (Programmable)	BPSK & QPSK	Viterbi	1/2 3/4 7/8	10^{-7}	6.7 8.0 9.0	3.5 to 4 dB	1–2 seconds	1–4 seconds	1–4 seconds	
Rec/Demod #2	9.6 kbit/s 2.048 Mbit/s	BPSK QPSK	Sequential	½ ¾	10^{-7}	5.6 6.4	3.4 to 4.2 dB	1–2 seconds	2–4 seconds	3–5 seconds	

ATTACHMENT 1 TO ANNEX 1

Sync. loss due to short term interference in an MPEG-2 digital video and audio receiver

1.0a Introduction

In this Attachment, the synchronization behavior of a digital video receiver is examined that is commonly used for satellite news gathering (SNG) and for video distribution by broadcasters. Similar complex receivers are also used for Direct to Home and BSS applications, data distribution, file transfer, broadcast of data, etc. This class of receiver was chosen for testing and evaluation because the video data is heavily coded and compressed where the loss of synchronization could cause long term outages. Other receivers designed for different types of service will perform similarly with different outage times.

2.0a Objective and approach

The objectives of the investigation were to determine the interference duration and the power level required that cause the receiver to lose lock and also to characterize the receiver outage time. For these measurements the interference is modeled as Gaussian noise. This is consistent with accepted test procedures that treat interference from digital sources. Measurements were obtained by raising the noise level to simulate the interference source. Initial tests were designed to characterize the BER performance of the receiver and were compared to the manufacturer's specifications in order to ensure that the system under test was performing properly. Additional tests were performed to determine the mean time to loss of lock, and the time for reacquisition. Tests were also conducted to determine the impact of noise bursts on receiver performance.

3.0a Receiver description

The digital video receiver under test integrates MPEG-2 digital video and MPEG-2 digital audio decoders into a single channel per carrier. That configuration allows direct reception of digitized video, audio, and data from satellite network transmissions. For this implementation the received signal was set as QPSK modulated where the receiver can handle data rates from 2.5 Mbit/s to 15 Mbit/s.

Figure 1 is a block diagram showing the receiver processing string. The received signal is demodulated, matched filtered and the detected symbols are quantized. The quantized symbols are convolutionally (Viterbi) decoded. The system can be setup for rate 1/2, 2/3, 3/4, 5/6, and 7/8 codes. The symbols then enter a Reed-Solomon (RS) decoder, and a de-interleaver that protects the RS decoder from burst errors generated by the Viterbi decoder. The RS decoder outputs MPEG-2 frames. These frames are decoded, demultiplexed and the MPEG-2 signal is converted to analogue TV format.

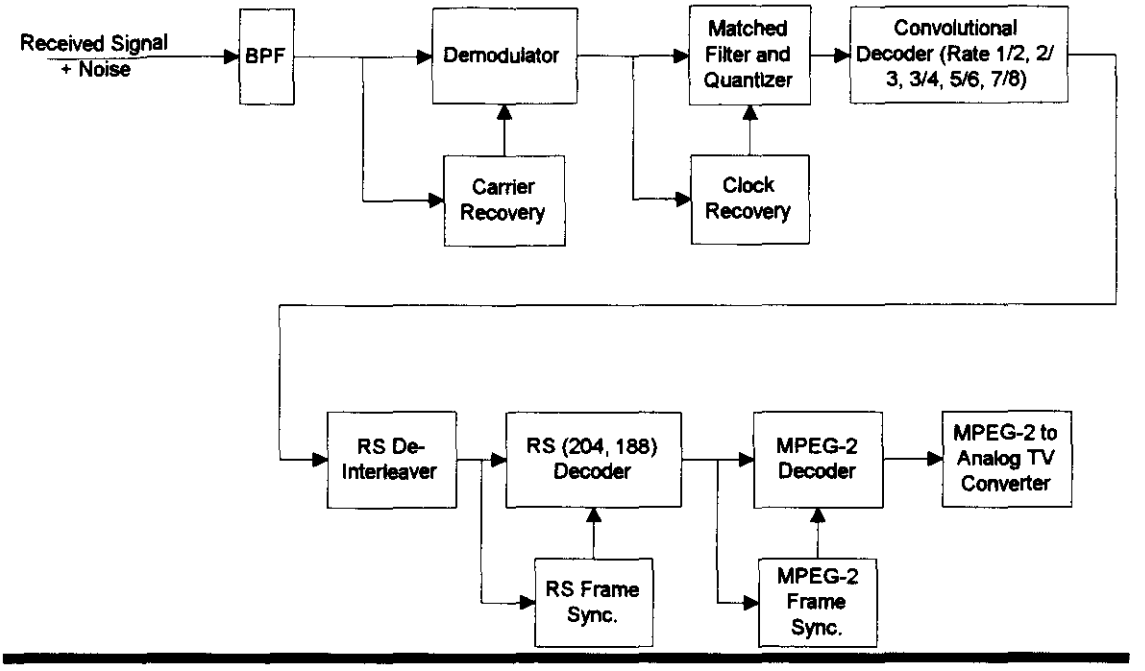

FIGURE A1

Digital video receiver block diagram

As seen in Figure A1, the receiver has many levels of synchronization from initial carrier recovery to MPEG-2 frame synchronization preceding conversion to Analogue TV. In general, higher level synchronization functions are more susceptible to loss of lock than the lower level functions. Therefore, frame and code synchronization will be lost before carrier synchronization. Loss of lock and reacquisition are primarily software functions. Thus the behaviour of the receiver can depend on the specific software implementation.

Figure A2 shows typical performance curves for the Reed-Solomon (RS) decoder for several different convolutional code rates. The clear sky performance threshold is usually set to the 10^{-10} BER point. This corresponds to an E_b/N_0=4.7 dB for a rate 1/2 code and an E_b/N_0=7.5 dB for a rate 7/8 code.

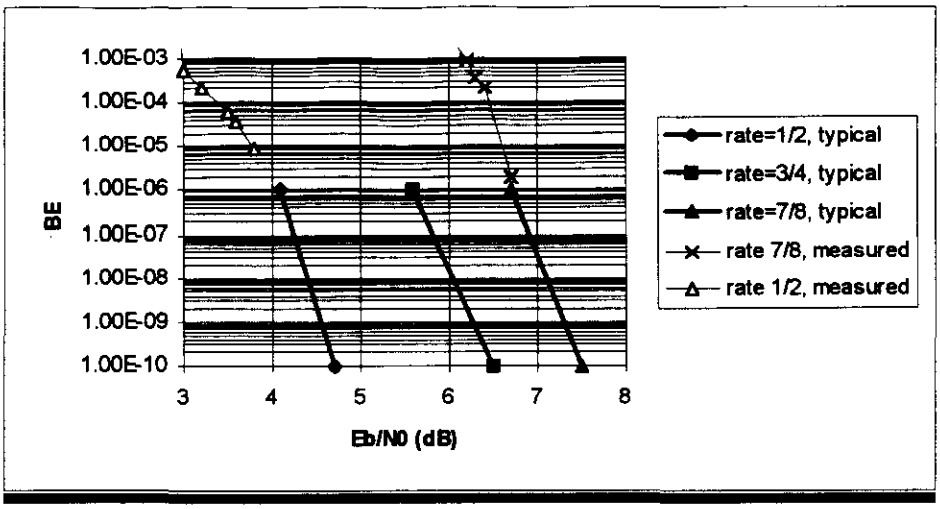

FIGURE A2

BER after the Reed-Solomon/Viterbi decoding

Fade thresholds are defined here as the minimum operating point for the receiver. Fade thresholds in satellite networks are often set for the 10^{-6} point. Table A1 presents E_b/N_0 fade thresholds for different convolutional code rates.

TABLE A1

Fade thresholds for error of 10^{-6}

Rate	½	2/3	3/4	5/6	7/8
E_b/N_0 dB	4	4.8	5.5	6.1	6.7

3.1a Receiver Performance

Figure A3 shows the BER test setup that used to verify the operation of the unit under test. The transmission rate was 3.68 Mbit/s. Two different code rates, 1/2 and 7/8, were tested. The performance of the receiver is included in Figure A2. Very low BERs were difficult to measure due to the burstiness of the channel. However, the results appear to agree with typical modem performance. The performance of this system was compared to other systems and the results were consistent to within 0.3 dB.

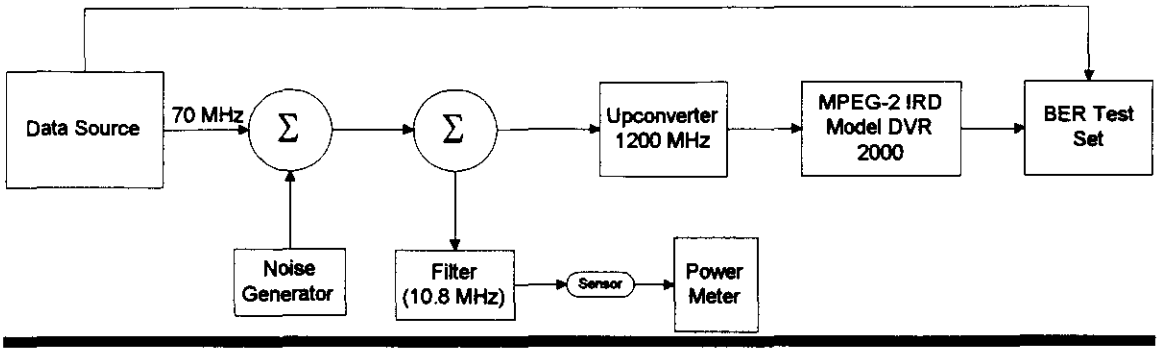

FIGURE A3

BER test setup

4.0a System test facility

Figure A4 shows the test setup used to test receiver synchronization behavior. The video source was program video of a sporting event. It was determined that the receiver performance was affected by the amount of motion in the video. That source was chosen because of its consistently erratic motion content that constantly stressed the video compression algorithms.

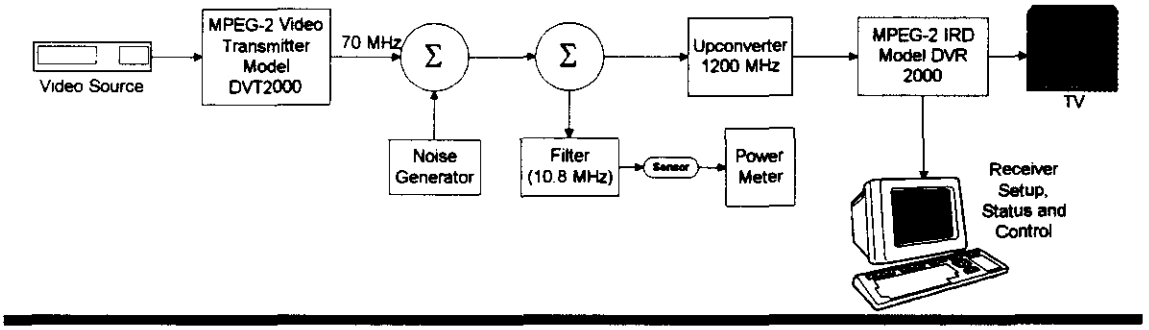

FIGURE A4

Video data test setup

Power meter measurements were made in terms of C/N and converted to E_b/N_0 using the following equation:

$$E_b/N_0 = C/N+10*\log((B_n/dr)=C/N+4.68 \quad (1)$$

where

B_n = the noise bandwidth = 10.8 MHz

dr = data rate = 3.68 Mbit/s.

The test receiver used, provided an external interface that allowed it to be controlled locally by a terminal. Diagnostics also can be made available for display on the terminal which include reports of the number of skipped and repeated frames that are printed every five seconds as well as indications of synchronization status. The test facility also included video displayed on a TV that provided a subjective indication of performance.

4.1a System test results

4.1.1a Loss of lock

Figures A5 and A6 show the number of frames lost as a function of E_b/N_0 for rate 1/2 and 7/8 codes, respectively. For each E_b/N_0 measurement point, results were averaged for 2 minutes. The steep excursion of the curves reflect the sensitivity of the concatenated convolutional / RS code. Below the E_b/N_0 point where the frame loss rate exceeds approximately 6 % the receiver loses lock. These correspond to a BER of about 10^{-3}.

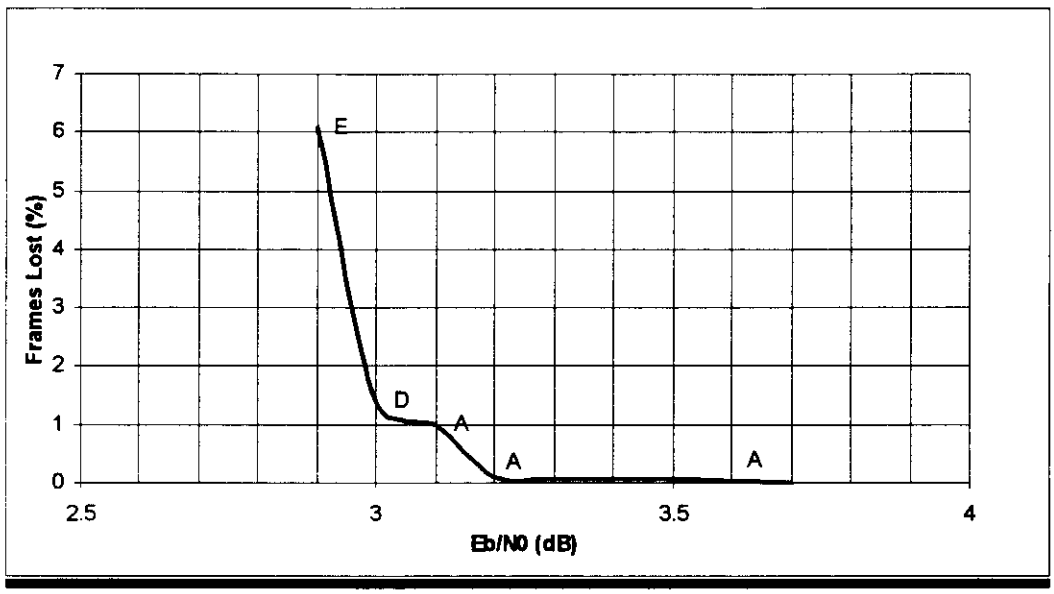

FIGURE A5

Percentage of video frames lost as a function of E_b/N_0 for the video receiver using rate ½ coding

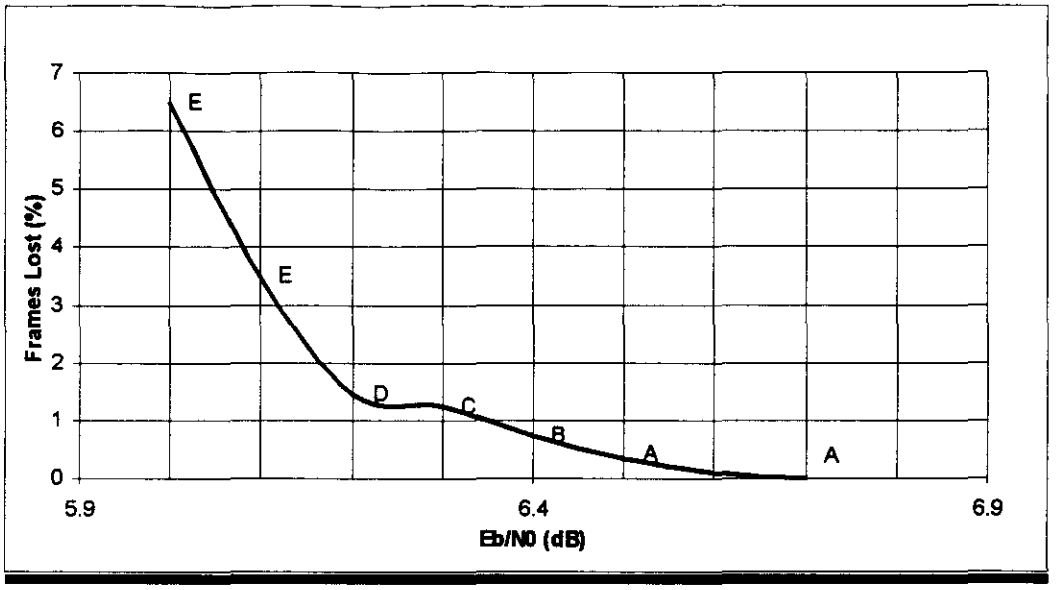

FIGURE A6

Percentage of video frames lost as a function of E_b/N_0 for the video receiver using rate 7/8 coding

By means of the TV monitor a subjective measurement on viewing quality was made. The subjective measurements are indicated by letters in Figures 5 and 6. The meaning of these letters is:

a) clear picture;

b) occasional jumps or error blocks in the picture;

c) frequent jumps or error blocks in the picture;

d) the picture is still viewable;

e) the picture is unviewable.

4.1.2a Mean time to loss of lock

The mean time to loss of lock was investigated for E_b/N_0 below the 6 % frame loss rate. Figures A7 and A8 show the mean time to loss of lock for rate 1/2 and 7/8 codes, respectively. These measurements were made by allowing the receiver lock up at a high E_b/N_0, then reducing the E_b/N_0 to the test value and recording the time it took to lose lock. Time measurements were made by viewing a clock. Ten measurements were averaged for each E_b/N_0.

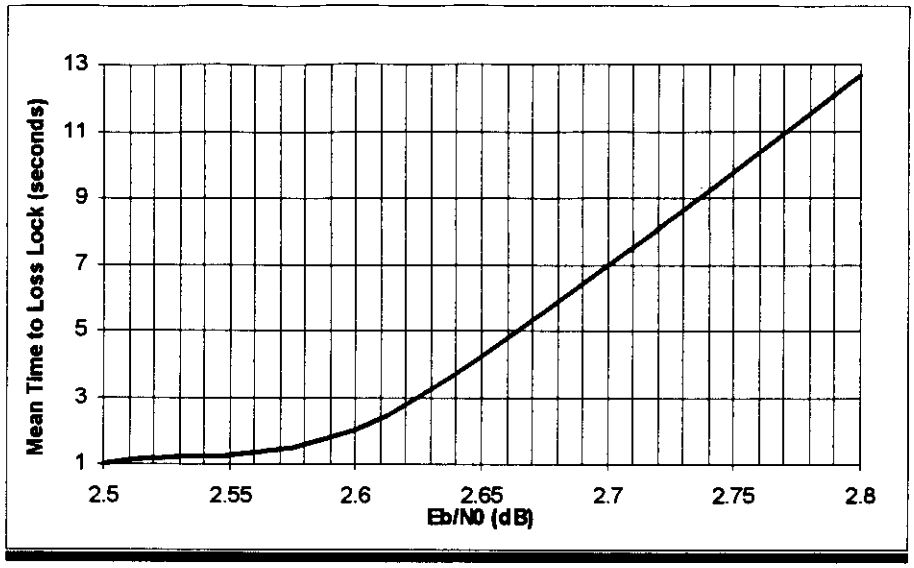

FIGURE A7

Mean time to loss of lock versus E_b/N_0 for the video receiver using ½ rate coding

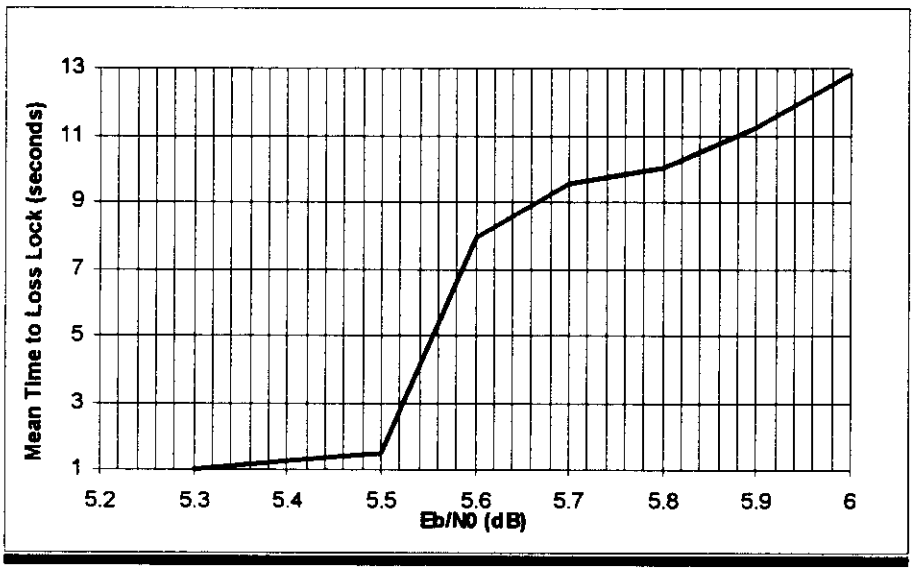

FIGURE A8

Mean time to loss of lock versus E_b/N_0 for the model video receiver using 7/8 rate coding

Below a certain E_b/N_0 the receiver always appears to lose lock in about one second. Since the interference from the NGSO system will occur in short bursts (on the order of seconds) this E_b/N_0 is critical. For the 1/2 rate coded system this E_b/N_0 is 2.5 dB and for the 7/8 coded system this E_b/N_0 is 5.3 dB. Relative to a 10^{-10} BER this corresponds to a 2.2 dB margin for both the 1/2 rate and 7/8 rate codes.

4.1.3a Reacquisition

For the receiver under test there are two search ranges for carrier lock. The initial acquisition uses a wide search mode that searches over a range of ± 1.5 MHz. Normal reacquisition uses a narrow search mode over a range of ± 140 kHz around the frequency it was last locked to. The receiver will remain in narrow search mode for approximately 5 minutes and if the carrier is not acquired it will switch to the wide search mode.

Since it is expected that NGSO interference will only cause short term bursts it can be assumed that reacquisition of the carrier is accomplished while in the narrow search mode. Time measurements indicate that reacquisition while in the narrow search mode takes approximately 4 seconds. Carrier search should only be a portion of this time because the search starts at the frequency where lock was lost. Most of the reacquisition time for the receiver involves re-initialization of internal programming.

An upgrade model of the tested digital video receiver promises performance that is slightly better than the tested version. However, this receiver has an additional 4 second delay built in before it starts the reacquisition process.

4.1.4a Recovery from interference bursts

This test is similar to the mean time to loss lock test described in Section 4.1.2a and better characterizes the impact of a burst of errors. Interference bursts were simulated by operating the receiver without noise and then switching a noise burst into the channel, for a short time. The noise burst was constrained to have an E_b/N_0=2.5 dB for the 1/2 rate coded channel and an E_b/N_0=5.3 dB for the 7/8 rate coded channel for a controlled time duration ±0.25 seconds. The results of this test are shown in Table A2.

This test indicates that it takes a burst duration of approximately 2 seconds to cause the receiver to lose lock, while, according to Section 4.1.2, the mean time to loss of lock occurred in just one second, for the same E_b/N_0. Apparently a low E_b/N_0 is required for more than one second to keep the channel from making a recovery.

TABLE A2

Receiver performance after being hit by a noise burst

Rate	E_b/N_0 transition level	Interference Duration	Loss of lock	Lost frames (%)
7/8	5.3	1	No	8.5
7/8	5.3	2	Yes	-
1/2	2.5	0.5	No	4.0
1/2	2.5	1	No	12
1/2	2.5	2	Yes	-

5.0a Conclusions

Performance measurements made on this receiver demonstrate a synchronization loss margin, compared to a 10^{-10} BER, of 2.2 dB. An interference burst of approximately 2 seconds is required to cause loss of lock and the receiver reacquires 4 seconds after the interference ends. Assuming a satellite channel has been implemented with margins that will protect during its availability to a threshold BER of 10^{-10}, then a receiver, in the circuit, of the type tested would lose lock if that margin was exceeded by 2.2 dB for a period of 1 to 2 seconds. Assuming operational levels were restored after loss of sync, the following receiver functions would reacquire in 4-8 seconds.